Contents lists available at SciOpen

Food Science and Human Wellness

journal homepage: https://www.sciopen.com/journal/2097-0765

China Food Publishing Co.

Tangeretin ameliorates abnormal irisin secretion in high-fat diet-induced obese mice *via* SESN2/AMPK/PGC-1α pathway

Jinjie Li[a,1], Jiangtao Li[a,1], Amin Ullah[b], Shuai Yao[a], Guangning Kou[a,b,*]

[a] *Centre for Nutritional Ecology and Centre for Sport Nutrition and Health, Zhengzhou University, Zhengzhou 450001, China*
[b] *Department of Nutrition and Food Hygiene, School of Public Health, Zhengzhou University, Zhengzhou 450001, China*

ARTICLE INFO

Article history:
Received 7 August 2024
Received in revised form 2 September 2024
Accepted 11 November 2024

Keywords:
Tangeretin
Irisin
FNDC5
Skeletal muscle

ABSTRACT

Irisin, a newly discovered myokine, plays an important role in maintaining energy balance and improving metabolic diseases. Tangeretin (TAN) is a natural active substance mainly found in the peel of citrus fruits, which has been reported to affect skeletal muscle function and prevent obesity-related metabolic diseases. However, the potential impact of TAN on the control of fibronectin type III domain-containing protein 5 (FNDC5)/irisin expression remains poorly understood. C2C12 cells, C57BL/6J mice, and HFD-induced obese mouse models were used in this study. Following treatment with TAN, the metabolic activity of mice was evaluated by metabolic cages, glucose tolerance test (GTT), and insulin tolerance test (ITT). Changes in relevant serum indices were detected by biochemical kits. The expression of FNDC5 *in vivo* and *in vitro* was examined by Q-PCR, Western blot, and immunostaining, and the binding effect of TAN and Sestrin2 (SESN2) was analyzed by molecular dynamics. We found that TAN treatment promoted irisin production and secretion in both C2C12 myotubular cells and C57BL/6J mice. The rise in irisin levels was found to be associated with the upregulation of FNDC5 expression, which was mediated *via* the SESN2/AMPK/PGC-1α signaling pathway. Moreover, this positive action by TAN was further verified in an obese mouse model induced by a high-fat diet (HFD). We found that TAN supplementation effectively resisted the decrease in circulating irisin levels and activated the SESN2 signaling axis expression in skeletal muscle, which may result in significantly improving metabolic parameters in HFD-fed mice. Our findings revealed that TAN counteracts the HFD-induced decrease in irisin secretion and improves glucose and lipid metabolism in obese mice by activating the SESN2/AMPK/PGC1-α/FNDC5 signaling axis. These findings present a novel opportunity for TAN to ameliorate irisin deficiency and other metabolic disorders.

1. Introduction

Skeletal muscle, comprising approximately 40% of total body weight, is the primary motor and metabolic organ in the human body. It serves vital functions in energy metabolism, maintaining internal balance, and promoting overall physical well-being[1]. Skeletal muscle has reemerged in the public perception as a secretory organ in recent years. The skeletal muscle can generate and secrete a diverse array of "muscle factors", which are integral to the body's life activities through the secretion mechanism[2]. Irisin is a newly identified muscle factor that is generated by the cleavage of fibronectin type III domain-containing protein 5 (FNDC5). FNDC5 is closely linked to muscle activity, and its expression is regulated by peroxisomal proliferator-activated receptor γ coactivator (PGC-1α)[3]. Recently, increasing reports shown that FNDC5/irisin expression activating exerts positive effects on regulating energy expenditure and improving metabolic homeostasis both *in vivo* and *in vitro* models[4-5]. Promoting irisin production and secretion has become an important way to prevent and improve obesity and obesity related metabolic diseases.

Exercise enhances the synthesis of PGC-1α and activation the expression of FNDC5, leading to an elevated secretion of irisin[6-8]. Although exercise is effective and beneficial, it may not be suitable for some people who have a physical challenge or over-obesity. Recently, studies reported that several natural products could

[1] These authors contributed equally to this work.
[*] Corresponding author at: Centre for Nutritional Ecology and Centre for Sport Nutrition and Health, Zhengzhou University, Zhengzhou 450001, China
E-mail address: kouguangning@zzu.edu.cn (G.N. Kou)
Peer review under responsibility of Beijing Academy of Food Sciences.

Publishing services by Tsinghua University Press

http://doi.org/10.26599/FSHW.2025.9250465

enhance skeletal function and activate FNDC5/irisin expression. For example, curcumin activated FNDC5/irisin expression to increase energy expenditure in high-fat diet (HFD)-fed mice and dihydromyricetin promoted irisin secretion both in rats and humans[4,9]. Tangeretin (TAN), a polymethoxy-flavone, abundant in citrus fruits and exhibits diverse pharmacological properties, including anti-inflammatory, antioxidant, anticancer, and neuroprotective effects[10-12]. It holds significant promise as a potential agent for addressing metabolic disorders like obesity and diabetes mellitus[13]. Previous research has demonstrated that TAN could exhibit a favorable impact on fat loss and metabolic parameter improvement in HFD-induced obese mice and TAN could regulate insulin sensitivity and the glucose homeostasis in *db/db* mice[14]. Besides, study showed that TAN could improve mitochondrial function and endurance capacity in skeletal muscle of mice[15]. However, it remains unclear whether TAN could exert positive effect by affecting the FNDC5 expression and irisin secretion.

In the present study, we aim to explore the potential action of TAN on regulating FNDC5/irisin expression both in C2C12 myotubles, C57BL/6J mice and HFD-fed obese mice, respectively. The irisin levels, FNDC5 expression, body weight gain, lean and fat mass, glucose levels, lipid profiles and energy expenditure as well as the potential mechanism were detected in these models.

2. Materials and methods

2.1 Cell culture and treatment

The C2C12 cells (Procell Life Science & Technology Co., Ltd., China) were cultivated in an incubator at 37 ℃ and 5% CO_2 in a growth medium prepared by adding 10% fetal bovine serum to DMEM high-sugar medium. Differentiation was initiated by adding a differentiation medium containing 2% horse serum when the cell fusion rate reached 80%–85%. To assess the impact of TAN on the expression of FNDC5/irisin *in vitro*. Differentiation was induced in C2C12 cells for 5 days; the cells were then treated for 24 h with TAN at concentrations of 0, 5, 10, and 20 μmol/L (HPLC ≥ 98.0%, Huike Botanical Development Co., Ltd., China).

2.2 Animal experiments

Male C57BL/6J mice, aged 8 weeks, were acquired from Beijing HFK Bioscience Co., Ltd. (No. 110322231103004381) and placed in College of Public Health's Medical Animal Center of Zhengzhou University. The mice were kept in a controlled environment with a 12 h light-dark cycle, maintaining a consistent ambient temperature of (23 ± 2) °C and humidity ranging from 50% to 60%. The Institutional Review Board for Life Sciences at Zhengzhou University approved all animal research (approval no: ZZURIB 2021-5302).

Protocol 1: The mice were randomly assigned to 3 groups of 10 mice each after they had been acclimatized in the new environment for 1 week. The control group (CON), 50 mg/kg TAN group (TAN50), and 100 mg/kg TAN group (TAN100) were all given free access to water and food (a standard diet, HFK, D1025). The mice in TAN group were orally administrated with different doses of TAN dissolved in 0.5% carboxymethylcellulose for 8 weeks. The mice in CON group were received a similar volume of vehicle.

Protocol 2: After acclimation, the mice were randomly assigned to 3 groups (n = 10): low-fat diet (LFD), HFD, and HFD+TAN group. The mice in the HFD+TAN group were provided with HFD (60 kcal% fat, D12492, Research Diets) and were daily given a dose of 100 mg/kg TAN for 8 weeks. The mice in the HFD group were provided with HFD (60 kcal% fat, D12492, Research Diets) and were also given an equal volume of vehicle. The mice in the LFD group were provided with low-fat diet (10 kcal% fat, D12450B, Research Diets) and were received an equal volume of vehicle. The food intake was recorded every 3 days and the body weight was monitored every week.

2.3 Metabolic cage test

The metabolic capacity of mice can be investigated by collecting data on their oxygen consumption (VO_2), energy expenditure (EE) and respiratory exchange rate (RER). The same number of mice from each group were randomly selected and placed in a comprehensive lab animal monitoring system (CLAMS, Columbus Instruments, USA) for testing. Before data collection, the mice were acclimatized to the new environment for 24 h. Meanwhile, the diet and environment of the mice should meet the requirements of the corresponding experimental conditions during the whole testing phase.

2.4 Body composition and magnetic resonance imaging (MRI) analysis

The total lean tissue mass and fat mass of mice were measured by a body composition analyzer (Niumag Corporation, China). MRI system then was used to scan the lean and fat distribution of the entire body. Niumag V3.0 MRI analysis software was carried out to deal with the original images.

2.5 Glucose tolerance test (GTT) and insulin tolerance test (ITT)

The mice were fasted for 12 h and administered 2.0 g/kg body weight glucose solution intraperitoneally to conduct the GTT[16]. For the ITT, the mice underwent fasting and were then injected with 0.75 U/kg body weight of insulin[17]. The mice were given access to water during the fasting period. Following glucose and insulin administrations, blood was collected from the tail, and the blood glucose levels were measured using a glucometer at various intervals (0, 15, 30, 60, 90, and 120 min). The area under the curve was calculated by plotting glucose tolerance and insulin tolerance curves based on the blood glucose values and the measurement time.

2.6 Enzyme-linked immunosorbent assay

Irisin concentrations were determined in serum and cell culture supernatant using an enzyme-linked immunosorbent assay kit following the manufacturer's instructions (Sino Best Biological Technology Co., Ltd., China).

2.7 Determination of blood lipid

The serum levels of triglyceride (TG), total cholesterol (TC), low-density lipoprotein-cholesterol (LDL-C), and high-density

lipoprotein-cholesterol (HDL-C) were measured in each group of mice according to the kit's instructions (Jiancheng Bioengineering Institute, Nanjing, China). The levels of each index in different groups of mice were recorded at particular wavelengths using the enzyme labeling apparatus.

2.8 Immunofluorescence and immunohistochemistry (IHC)

Immunofluorescence: C2C12 cells were fixed with 4% paraformaldehyde and permeabilized with 0.5% Triton X-100 for 15 min after being induced to differentiate and treated with TAN. Next, the cells were closed in a 3% BSA solution for 30 min. Subsequently, the cells were treated with the primary antibody (FNDC5, 1:300, Proteintech) overnight at 4 °C. The following day, upon incubation of the secondary antibody (IgG H&L/FITC, 1:400, Abcam) at room temperature, the nuclei were stained with DAPI solution and photographed under a microscope.

IHC: After pre-paraffin embedding, the gastrocnemius and soleus muscles were sectioned into 5 μm thick slices. Subsequently, the sections were closed in 10% goat serum and incubated with FNDC5 antibody (FNDC5, 1:300, Proteintech) for 12 h following antigen recovery and endogenous peroxidase quenching. The sections were incubated with secondary antibodies and photographed under a microscope following the completion of these manipulations. Staining results were measured and analyzed by ImageJ software.

2.9 Western blotting (WB) analysis

Total proteins from muscle tissues and cells were extracted using RIPA lysate mixed with protease inhibitors (Beyotime, China), and their protein concentrations were detected using a BCA assay kit (Beyotime, China). The denatured proteins were evenly divided, placed into SDS-PAGE gels, and transferred onto PVDF membranes using a wet-transfer method. The membranes were immersed in 5% BSA at room temperature for 2 h, followed by incubation with the primary antibodies at 4 °C for 12 h (AMPK (1:5 000); PGC-1α (1:5 000); FNDC5 (1:3 000); GAPDH (1:5 000); Sestrin2 (SESN2) (1:5 000) (Proteintech, Wuhan, China); p-AMPK (1:2 500) (Cell Signaling Technology, Massachusetts, USA). Subsequently, the membranes were incubated with the secondary antibodies at room temperature for 1 h. Luminescence was detected to visualize protein signals, and protein expression was analyzed with the help of ImageJ software.

2.10 Quantitative real-time PCR (Q-PCR)

The RNA was isolated using a TRIzol reagent (Invitrogen, USA) and the extracted RNA was synthesized into cDNA using PrimeScript RT kit reagents (Takara, Japan). The Q-PCR reaction was run in a Bio-Rad CFX96TM real-time system using SYBR Green Mix. The $2^{-\Delta\Delta CT}$ method was used to determine the level of *FNDC5* mRNA expression. Specific primer-targeting gene sequences are listed below, *FNDC5*: 5′-TGCAGGCCATCTCCATCCAG-3′ (forward) and 5′-GGCCATCTTTTCAGCCTCGC-3′ (reverse); *36B4*: 5′-GCTTCGTGTTCACCAAGGAGGAC-3′ (forward) and 5′-GTTCTGAGCTGGCACAGTGACC-3′ (reverse).

2.11 Molecular docking and molecular dynamics (MD) simulations

The structures of SESN2 and TAN were retrieved from the RCSB PDB (ID: 5t0n) and PubChem databases, respectively. AutoDock Vina 1.1.2 was used to perform molecular docking of SESN2 and TAN. The best-docked conformation was used for subsequent MD simulations. MD simulations were conducted with AMBER software[18]. The system was subjected to an energy minimization analysis before the simulation, which involved the conjugate gradient method with 2 500 steps and the steepest descent method with 2 500 steps. During the energy minimization procedure, the system temperature was systematically raised from 0 to 298.15 K for 200 ps. The simulation was conducted using the NVT (isothermal-isovolumetric) ensemble at a constant temperature of 298.15 K. Following that, the entire system underwent a simulation in equilibrium for 500 ps at NPT (isothermal-isobaric) conditions. Ultimately, 2 composite systems were subjected to 100 ns NPT ensemble simulations while adhering to periodic boundary conditions. The Particle Mesh Ewald (PME) method calculates long-range electrostatic interactions within a truncation range of 10 Å[19]. The SHAKE approach was employed to constrain the bond lengths of the hydrogen atoms, while the Langevin algorithm was utilized for temperature regulation[20-21]. The system was maintained at a pressure of 1 atm, using a time step of 2 fs. Traces were captured every 10 ps for further examination. The protein-ligand binding free energy was computed using the MM/GBSA approach[22-24]. The computations were performed using the following equations with MD trajectories of 90–100 ns at coordinates:

$$\Delta G_{\text{bind}} = \Delta G_{\text{complex}} - (\Delta G_{\text{receptor}} + \Delta G_{\text{ligand}})$$
$$= \Delta E_{\text{internal}} + \Delta E_{\text{vdW}} + \Delta E_{\text{elec}} + \Delta G_{\text{GB}} + \Delta G_{\text{SA}}$$

Where ΔE_{vdW}, ΔE_{elec}, ΔG_{GB}, ΔG_{SA}, and ΔG_{bind} represent the van der Waals energy, electrostatic energy, electrostatic contribution to solvation, nonpolar contribution to solvation, and binding free energy, respectively. This study used the single trajectory technique to eliminate the $\Delta E_{\text{internal}}$ between the complex, receptor, and ligand. This cancellation effectively reduces noise levels in most circumstances. The absence of entropy changes results from significant computing resource usage with low accuracy[23].

2.12 Statistical analysis

IBM SPSS statistics 21 software and GraphPad Prism 8.0 were used to perform statistical analysis. The result was expressed as the mean ± SD. One-way ANOVA and Student's *t*-test were used to analyze statistical significance among groups. $P < 0.05$ was regarded as a statistically significant threshold.

3. Results

3.1 TAN treatment promotes FNDC5/irisin expression in C2C12 myotubes

The impact of TAN on irisin levels was initially identified in C2C12 myotubes. Fig. 1A demonstrates that TAN administration effectively stimulated the expression of *FNDC5* mRNA in C2C12 myotubes compared to the control group, as indicated by the Q-PCR

result ($P < 0.05$). The WB and immunofluorescence results confirmed that TAN therapy significantly increased the expression of the FNDC5 protein in C2C12 myotubes compared to the control group ($P < 0.05$) (Figs. 1B-E). Furthermore, the ELISA results showed a significant elevation in irisin levels in C2C12 myotubes following TAN treatment compared to the control group ($P < 0.05$) (Fig. 1F). Our result suggests that TAN can enhance the expression of FNDC5 and the release of irisin in C2C12 myotubes.

3.2 TAN supplementation increases irisin secretion in mice

Subsequently, the impact of TAN on irisin was examined in C57BL/6J mice. According to Figs. 2A-D, there were no significant differences in body weight, average food consumption, and lean mass between the control group and the group of mice who received TAN supplementation. Interestingly, our findings indicate that the administration of TAN slightly decreased fat mass in mice compared to the untreated group (Fig. 2E). The Q-PCR results showed that the expression of *FNDC5* mRNA in the soleus and gastrocnemius muscle of mice was activated by TAN supplementation in comparison to the control group ($P < 0.05$) (Figs. 2F and G). Furthermore, the WB and IHC results showed that TAN increased the expression of FNDC5 protein in mice's soleus and gastrocnemius muscle ($P < 0.05$) (Figs. 2I-N). According to these findings, the serum irisin levels of the TAN50 and TAN100 group mice were significantly elevated compared to those of the control group mice ($P < 0.05$) (Fig. 2H). These data collectively suggested that TAN could enhance the expression of FNDC5/irisin in mice.

3.3 TAN stably bound to SESN2 protein

Several studies have reported that SESN2 is a significant upstream regulator that influences the expression of PGC-1α[25-26], a crucial factor in enhancing muscle fitness. Recently, there has been increasing evidence that molecular docking and MD modeling are highly efficient in predicting drug and protein binding[27-29]. Our docking results indicate that TAN can form a strong binding affinity with SESN2 protein, primarily through hydrophobic interaction and hydrogen bonding (Figs. 3A and B). The structural and energetic changes during TAN and SESN2 protein binding were thoroughly investigated using MD simulation to assess the TAN-SESN2 binding properties further. As shown in Fig. 3C, the root mean square deviation (RMSD) value of SESN2 protein did not fluctuate significantly after 40 ns, establishing a more reliable foundation for the binding of TAN. Similarly, the RMSD value of TAN reached a stable fluctuation after 40 ns (Fig. 3C), suggesting that TAN is stable in the SESN2 protein pocket. As shown in Fig. 3D, the binding sites of TAN are similar at the initial (0 ns) and final (100 ns) moments of the simulation. However, the SESN2 protein pocket encases TAN more tightly at the final moments (100 ns), which is consistent with the fluctuation data we observed in the RMSD data. This implies that the TAN binding may become more stable at a later stage of the simulation.

We utilized the MM/GBSA method to determine the binding energy by analyzing the MD simulation trajectory. This approach provides a more precise representation of the interaction between the small molecule

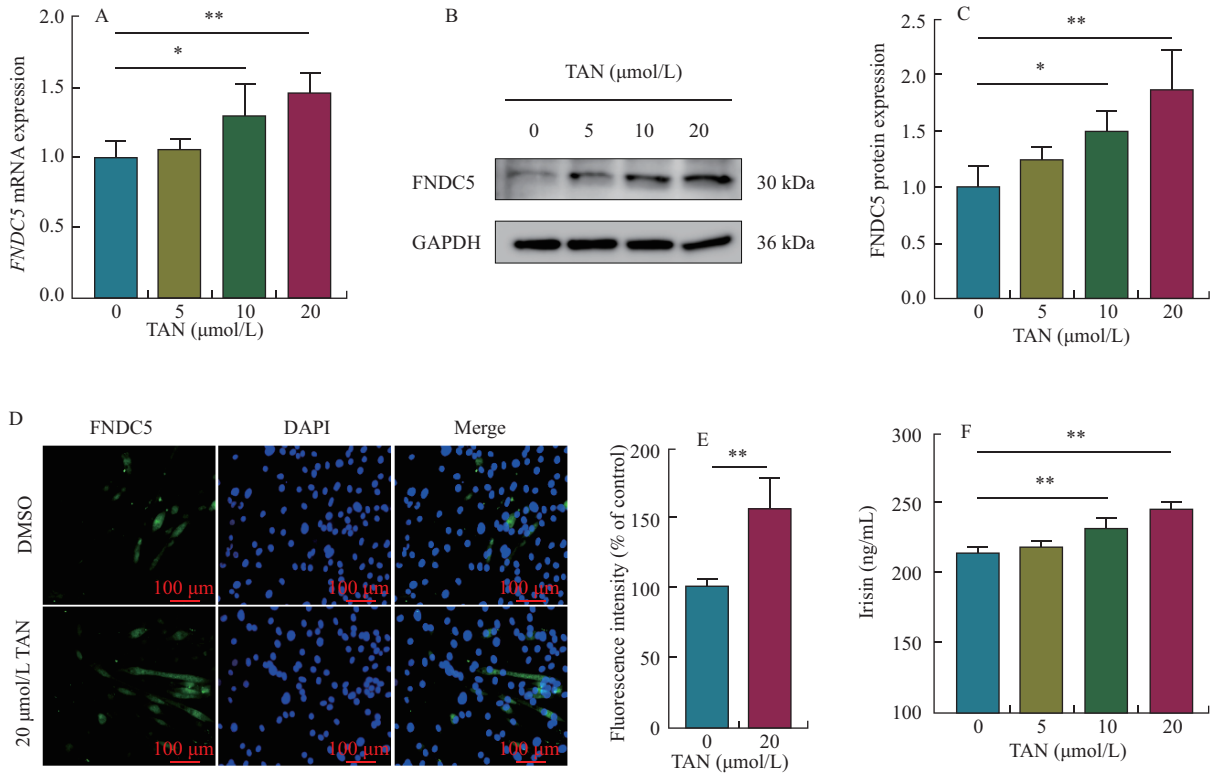

Fig. 1 TAN treatment promotes FNDC5/irisin expression in C2C12 myotubes. (A) The expression of *FNDC5* gene in C2C12 myotubes ($n = 5$). (B and C) WB analysis of FNDC5 protein in C2C12 myotubes ($n = 4$). (D and E) FNDC5 immunofluorescence analysis in C2C12 myotubes ($n = 3$). (F) Irisin levels in C2C12 myotubes ($n = 6$). Data are expressed as mean ± SD. *$P < 0.05$; **$P < 0.01$.

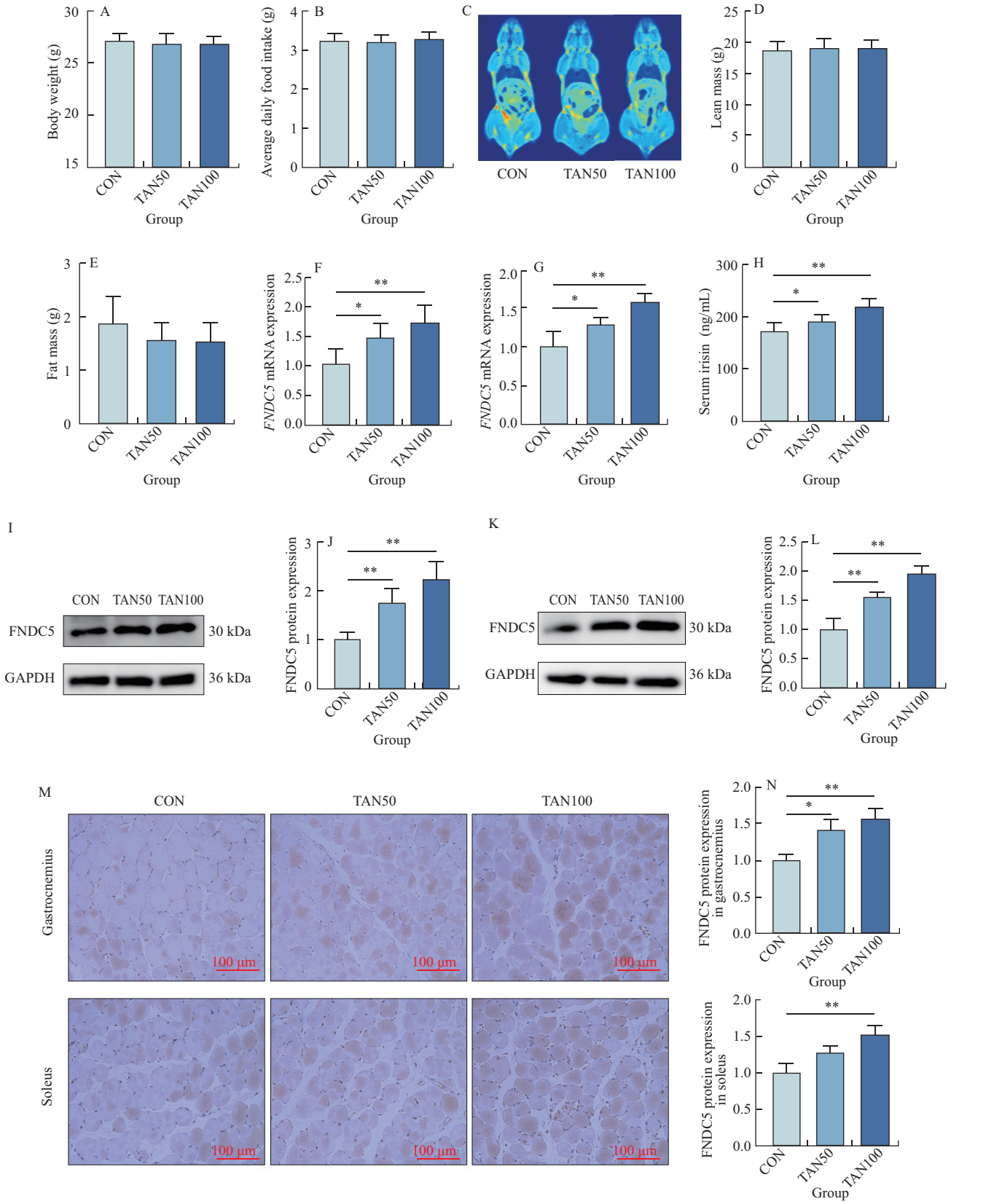

Fig. 2 TAN supplementation increases irisin secretion in mice. (A) Body weight ($n = 10$). (B) Average daily food intake ($n = 10$). (C) Magnetic resonance imaging. (D and E) Lean and fat mass ($n = 6$). *FNDC5* mRNA expression in (F) gastrocnemius and (G) soleus muscles ($n = 5$). (H) Serum irisin levels of mice ($n = 8$). WB analysis of FNDC5 protein in (I-J) gastrocnemius and (K-L) soleus muscles ($n = 4$). (M and N) IHC analysis of FNDC5 in gastrocnemius and soleus muscles ($n = 3$). Data are expressed as mean ± SD. $^*P < 0.05$; $^{**}P < 0.01$.

and the target protein[30]. As shown in Fig. 3E, the binding energy of TAN-SESN2 is (–36.58 ± 2.70) kcal/mol. Negative values signify the presence of binding affinity between small molecules and the target protein, with lower values indicating a stronger interaction. Our estimates indicate that TAN-SESN2 has a high level of binding affinity. An energy decomposition analysis reveals that the main contributor to the binding of TAN and SESN2 is van der Waals energy, followed by electrostatic energy, and finally, nonpolar solvation free energy (Fig. 3E). Furthermore, the top 10 amino acids contributing to TAN and SESN2 binding were identified as ILE378, LEU389, THR374, TYR375, PHE447, ALA379, ARG448, TRP444, THR386, and ASN376 using the energy decomposition technique (Fig. 3F). These data suggest that TAN exhibits a consistent and stable binding affinity towards the SESN2 protein.

3.4 TAN activates SESN2/AMPK/PGC-1α pathway in C2C12 myotubes and mice

To examine the potential mechanism by which TAN affects the expression of FNDC5/irisin, we investigated the SESN2/AMPK/PGC-1α axis in both C2C12 cells and the skeletal muscle of mice. In our study on C2C12 myotubes, we observed that treatment with TAN resulted in a considerable increase in the expression of SESN2, p-AMPK/AMPK, and PGC-1α proteins compared to the control group ($P < 0.05$) (Figs. 4A and B). TAN consistently increased the expression of SESN2, p-AMPK/AMPK, and PGC-1α proteins in the gastrocnemius muscle of mice ($P < 0.05$) (Figs. 4C and D). TAN exhibited a notable activation of the SESN2/AMPK/PGC-1α axis in the soleus muscle of mice in comparison to the control group ($P < 0.05$) (Figs. 4E and F). These observations suggest that TAN can activate the SESN2/AMPK/PGC-1α pathway both *in vivo* and *in vitro*.

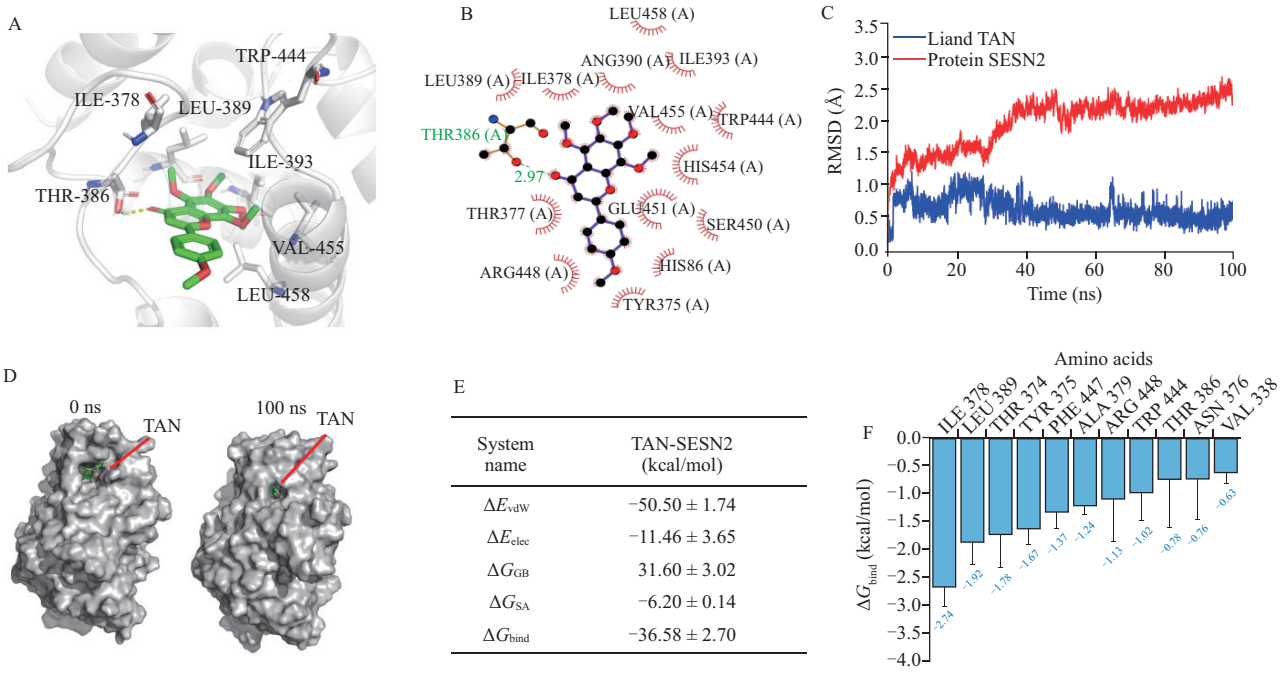

System name	TAN-SESN2 (kcal/mol)
ΔE_{vdW}	−50.50 ± 1.74
ΔE_{elec}	−11.46 ± 3.65
ΔG_{GB}	31.60 ± 3.02
ΔG_{SA}	−6.20 ± 0.14
ΔG_{bind}	−36.58 ± 2.70

Fig. 3 TAN stably bound to SESN2 protein. (A and B) Binding modes of TAN to the SESN2 protein in 3D and 2D. (C) Changes in the RMSD of the TAN and SESN2 during MD simulations. (D) Conformational changes of TAN-SESN2 before and after MD simulation. (E) Binding free energies and energy components predicted by MM/GBSA. (F) The top 10 amino acids based on energy contribution to TAN binding to SESN2.

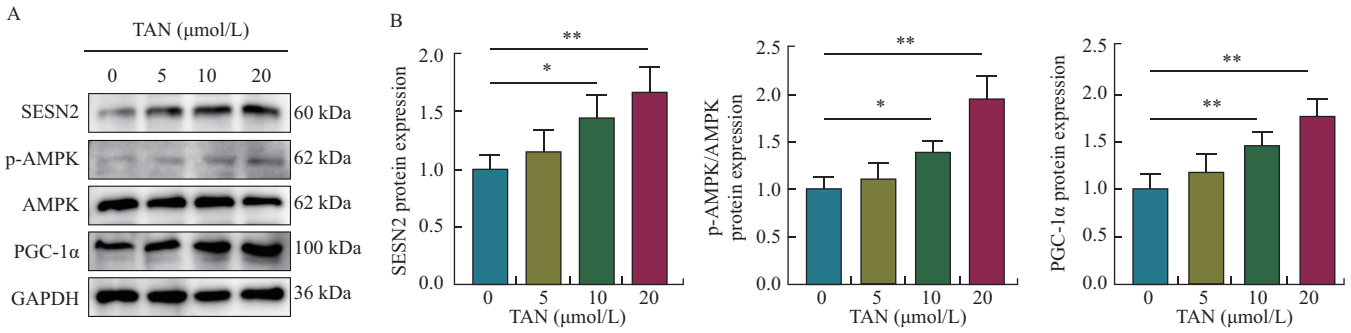

Fig. 4 TAN activates SESN2/AMPK/PGC-1α pathway in C2C12 myotubes and mice. (A and B) WB analysis of SESN2, p-AMPK/AMPK, and PGC-1α in C2C12 myotubes ($n = 4$). (C and D) WB analysis of SESN2, P-AMPK/AMPK, and PGC-1α in gastrocnemius muscle ($n = 4$). (E and F) WB analysis of SESN2, p-AMPK/AMPK, and PGC-1α in soleus muscle ($n = 4$). Data are expressed as mean ± SD. *$P < 0.05$; **$P < 0.01$.

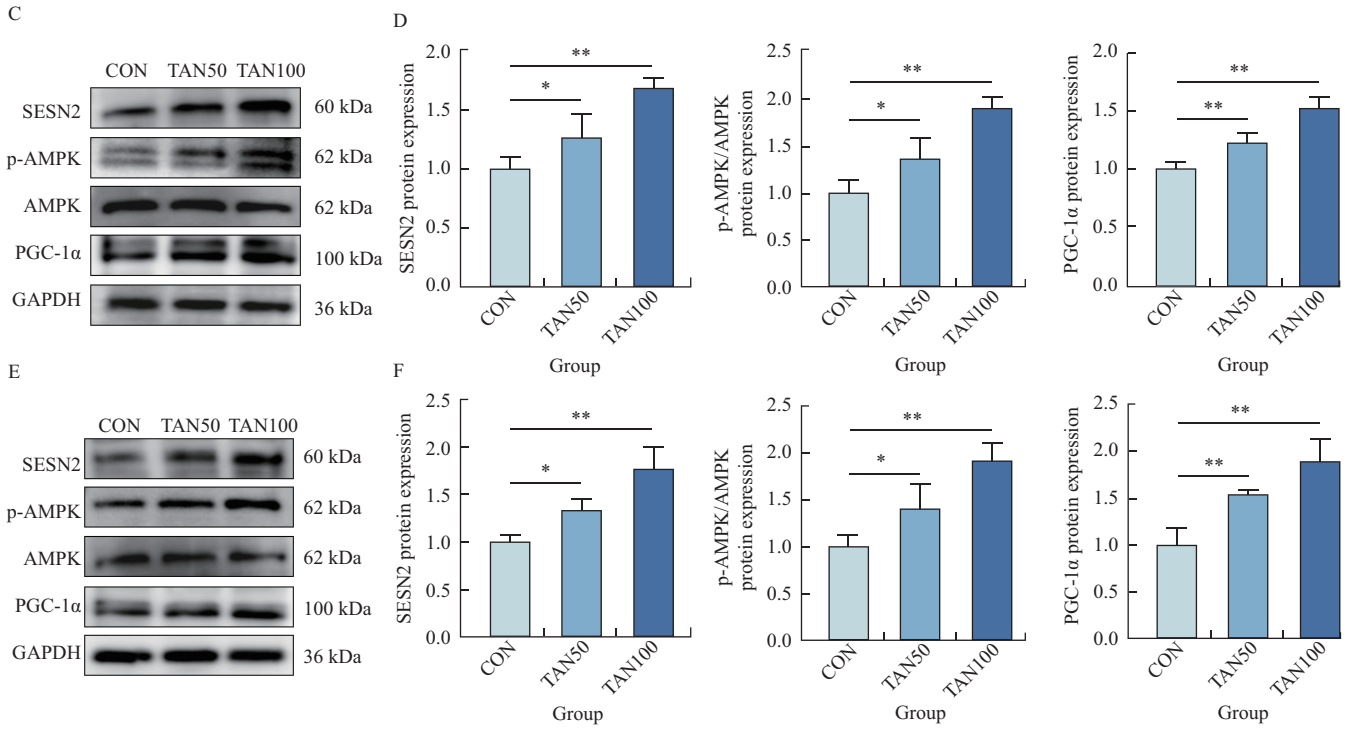

Fig. 4 (*Continued*)

3.5 TAN improves metabolic parameters in HFD-fed mice

According to recent research, improvements in metabolic parameters are closely associated with elevated levels of circulating irisin[5,31-32]. We investigate whether TAN can mitigate the altered metabolic parameters induced by HFD in mice. In comparison to the HFD group, TAN supplementation significantly reduced HFD-induced increases in body weight and fat mass ($P < 0.05$) and slightly increased lean mass, as shown in Figs. 5A-D. Meanwhile, the serum levels of TC ($P < 0.05$), TG ($P < 0.05$), and LDL-C ($P < 0.05$) in the HFD+TAN group mice were lower than those of the HFD group mice, while HDL-C did not show significant changes (Figs. 5E-H). In addition, TAN supplementation significantly reduced the blood glucose levels during the GTT test compared to the HFD group ($P < 0.05$) (Figs. 5I and J). Similarly, TAN supplementation significantly reduced the glucose levels during the ITT test compared to the HFD group ($P < 0.05$) (Figs. 5K and L). These data suggested that TAN could improve glucose and lipid metabolism disorders in HFD-fed mice.

3.6 TAN regulates metabolic rate in HFD-fed mice

Next, the impact of TAN on metabolic rate was examined in mice that were administered a high-fat diet. In comparison to the LFD group, the mice in the HFD group exhibited a lower VO_2 ($P < 0.05$) and EE ($P < 0.05$) (Figs. 6A-B and E-F). However, the mice in the HFD+TAN group exhibited a significant increase in VO_2 ($P < 0.05$) and EE ($P < 0.05$) and a decrease in RER ($P < 0.05$) compared to the HFD mice (Figs. 6A-F), suggesting an upregulated lipid metabolism in the HFD+TAN group mice. Together, these data indicate that TAN can significantly reverse the reduction in metabolic rate induced by HFD in mice.

3.7 TAN improves the decrease of FNDC5/irisin expression in HFD-fed mice

Previous research has shown that mice fed HFD had lower circulating irisin levels than those maintained on a control diet[4,31-32]. We subsequently investigated whether TAN could enhance the expression of FNDC5 and circulating irisin levels in HFD-fed mice. Our findings revealed a substantial drop in blood irisin levels in the HFD group compared to the LFD group ($P < 0.05$) (Fig. 7A). However, supplementation with TAN considerably reversed the decrease in irisin secretion induced by the HFD group ($P < 0.05$) (Fig. 7A). In addition, TAN activated FNDC5 expression in the soleus and gastrocnemius muscles compared to the HFD group, as indicated by Q-PCR, WB, and IHC ($P < 0.05$) (Figs. 7B-I). Together, these data indicated that TAN could activate FNDC5/irisin expression in HFD-fed mice.

3.8 TAN activates SESN2 signaling axis in HFD-fed mice

The SESN2/AMPK/PGC-1α pathway was also examined in the soleus and gastrocnemius muscles of HFD-fed mice to determine whether the SESN2 signaling axis was involved in the TAN-induced FNDC5/irisin expression. The SESN2 and PGC-1α expression and p-AMPK/AMPK ratio in HFD group mice were significantly lower than in the LFD group ($P < 0.05$) (Figs. 8A-D). The gastrocnemius muscle of the HFD + TAN group mice exhibited a significant increase in the expression of SESN2, p-AMPK/AMPK, and PGC-1α compared to the HFD group mice ($P < 0.05$) (Figs. 8A and B). Additionally, the expression of SESN2 signaling axis-related proteins was significantly up-regulated in the soleus muscle of HFD+TAN group mice ($P < 0.05$) (Figs. 8C and D). Overall, these findings suggested that TAN could activate the SESN2/AMPK/PGC-1α pathway in the skeletal muscle of HFD-fed mice.

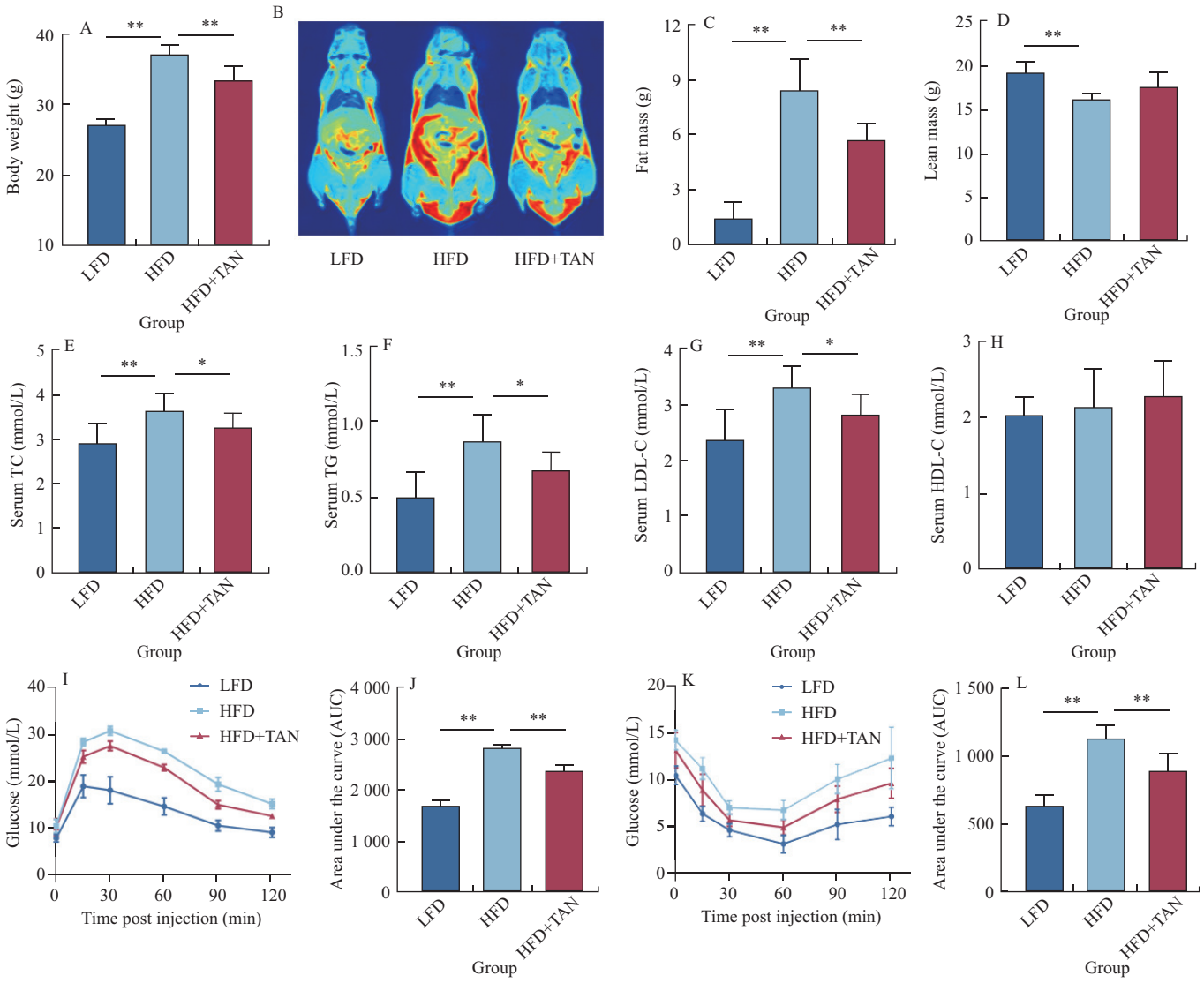

Fig. 5 TAN improves metabolic parameters in HFD-fed mice. (A) Body weight (n = 10). (B) Magnetic resonance imaging. (C and D) Fat and lean mass (n = 6). (E-H) Serum concentrations of TC, TG, LDL-C, and HDL-C (n = 8). (I and J) GTT (n = 6). (K and L) ITT (n = 6). Data are expressed as mean ± SD. *P < 0.05; **P < 0.01.

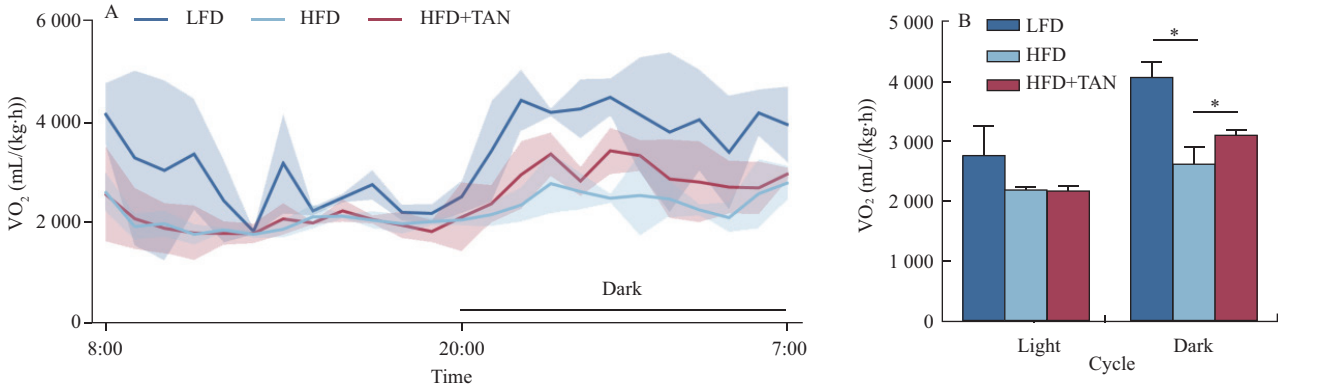

Fig. 6 TAN regulates metabolic rate in HFD-fed mice. (A and B) VO_2 in 24 h light-dark cycle (n = 3). (C and D) RER in 24 h light-dark cycle (n = 3). (E and F) EE in 24 h light-dark cycle (n = 3). VCO_2: carbon dioxide production. Data are expressed as mean ± SD. *P < 0.05; **P < 0.01.

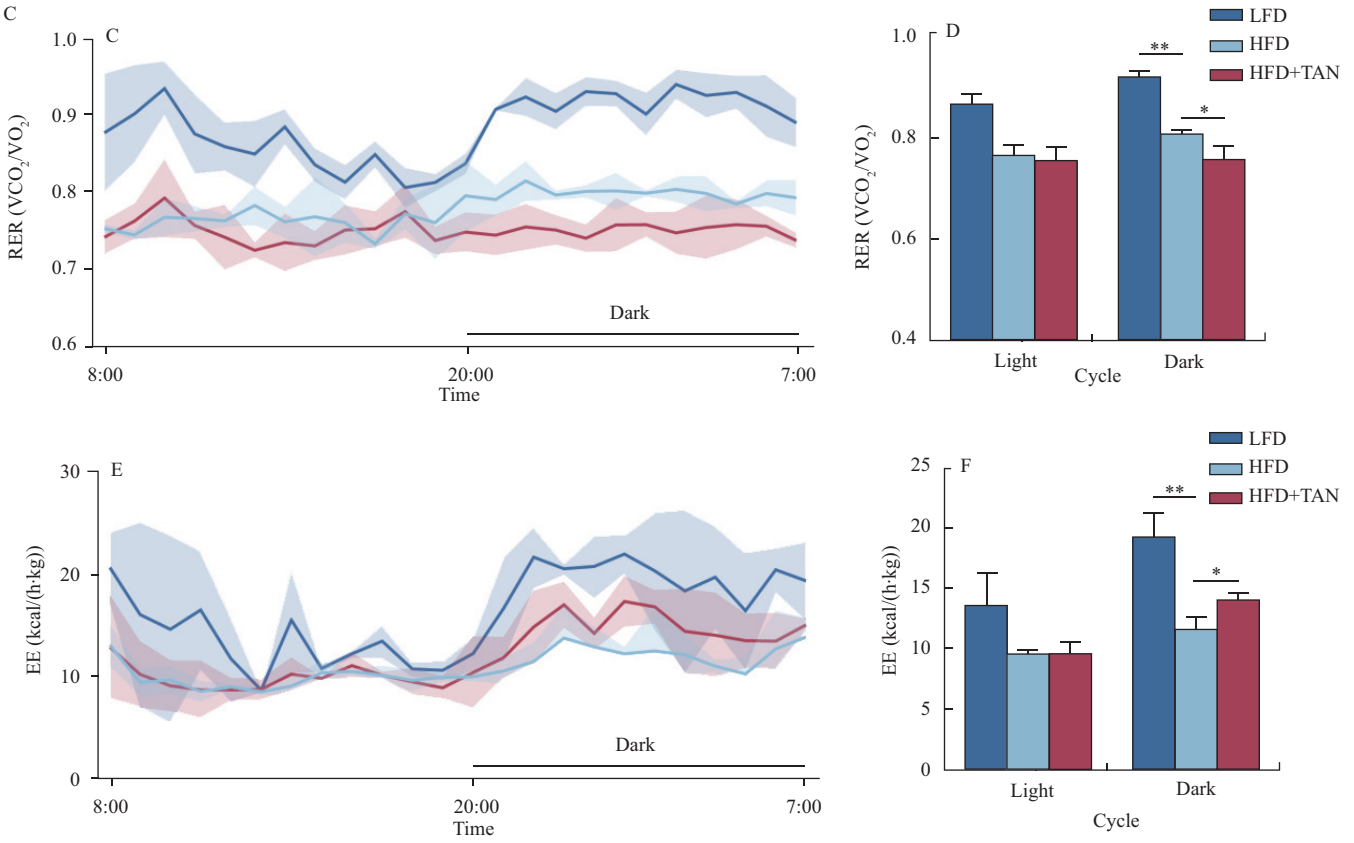

Fig. 6 (*Continued*)

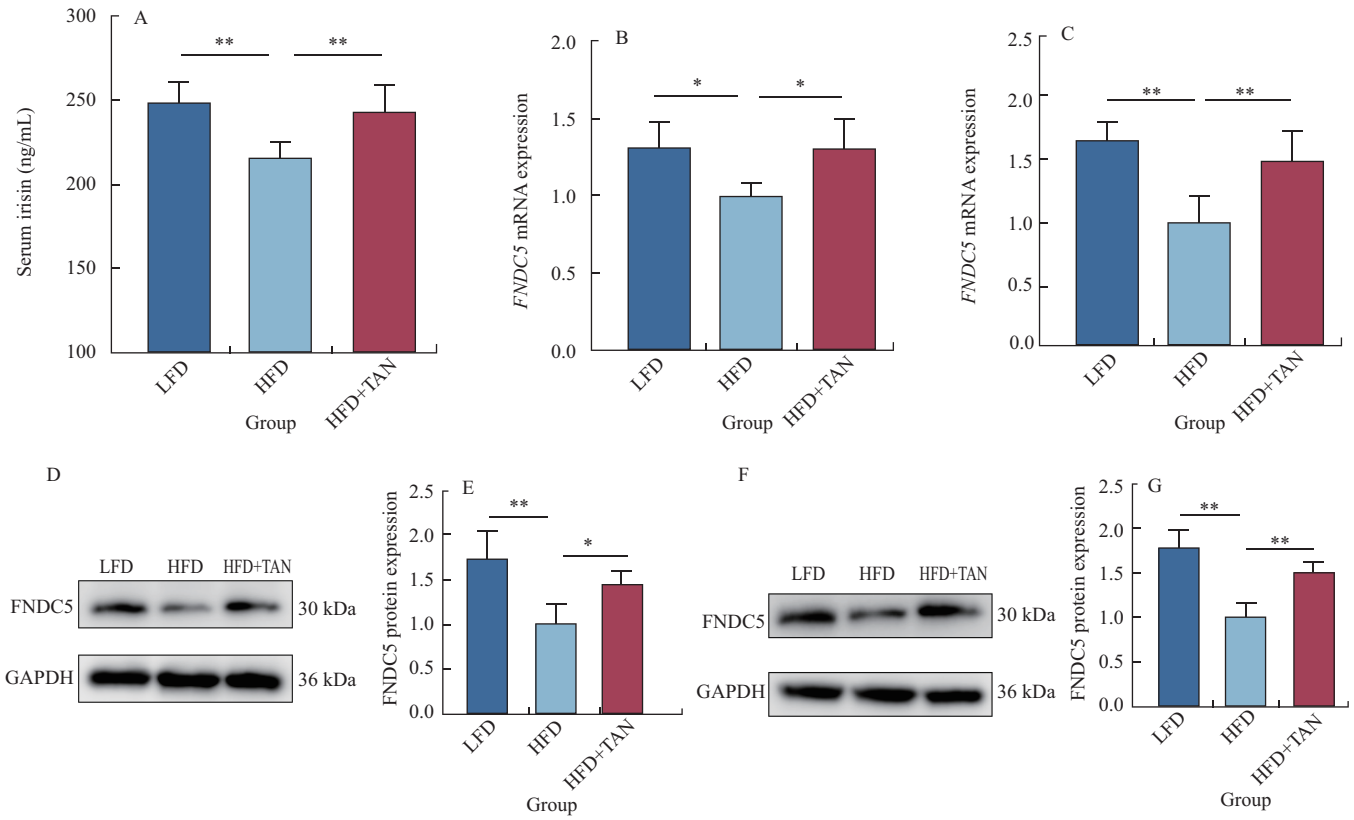

Fig. 7 TAN improves the decrease of FNDC5/irisin expression in HFD-fed mice. (A) Serum irisin levels of mice (n = 8). *FNDC5* mRNA expression in (B) gastrocnemius and (C) soleus muscles (n = 5). WB analysis of FNDC5 protein in (D-E) gastrocnemius and (F-G) soleus muscles (n = 4). (H and I) IHC analysis of FNDC5 in gastrocnemius and soleus muscles (n = 3). Data are expressed as mean ± SD. *P < 0.05; **P < 0.01.

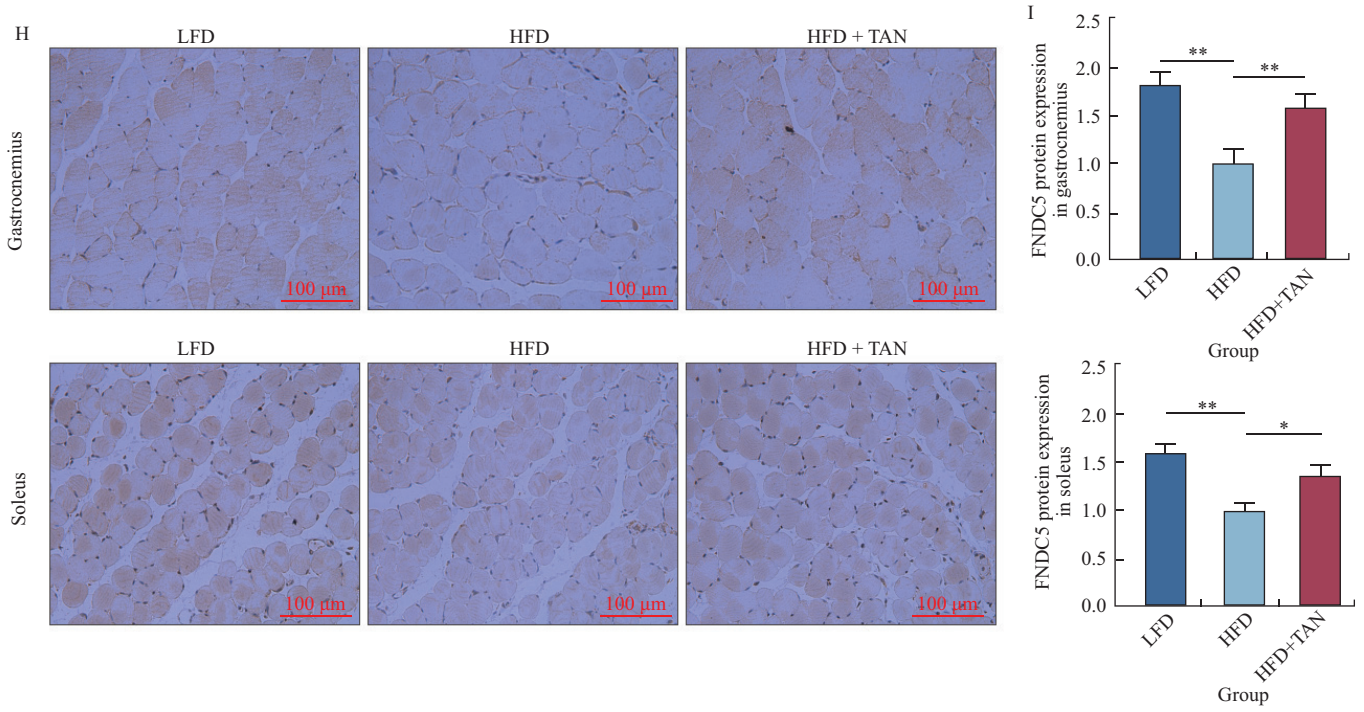

Fig. 7 (*Continued*)

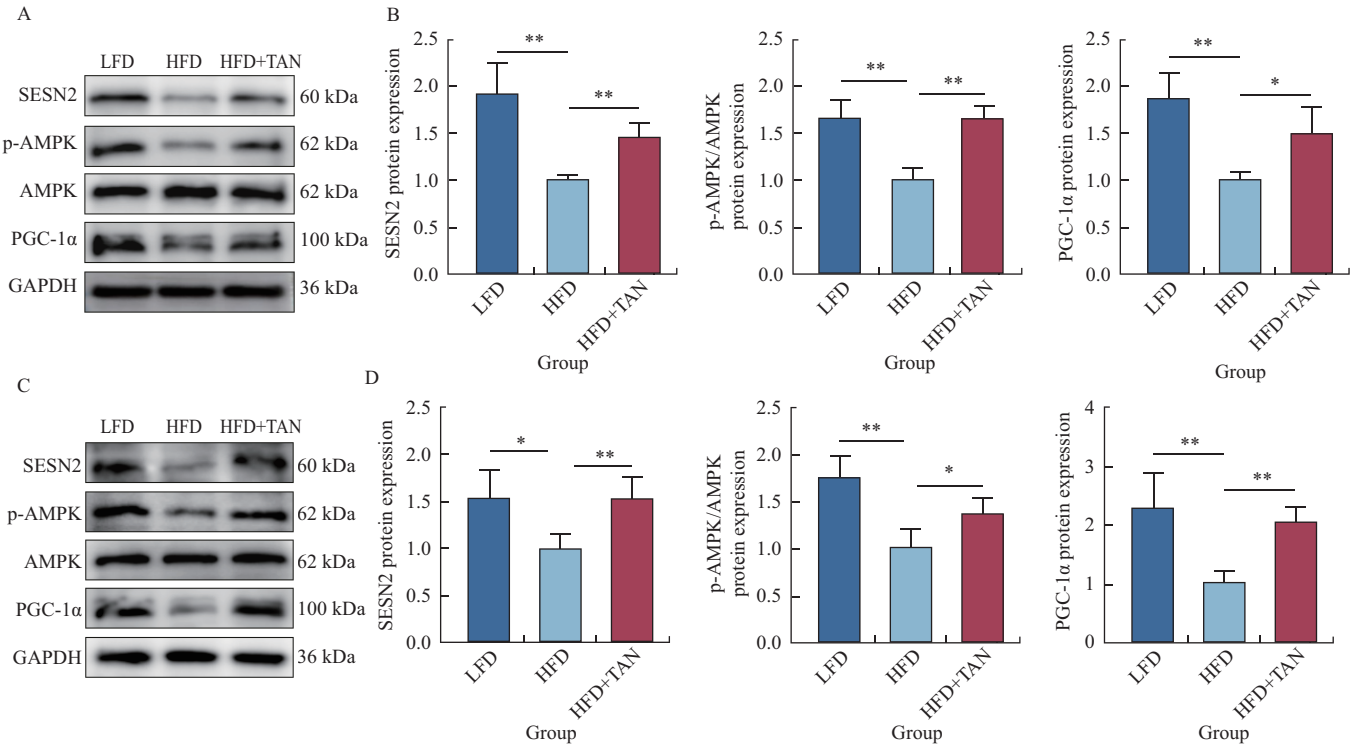

Fig. 8 TAN activates SESN2 signaling axis in HFD-fed mice. (A and B) WB analysis of SESN2, p-AMPK/AMPK, and PGC-1α in gastrocnemius muscle ($n = 4$). (C and D) WB analysis of SESN2, p-AMPK/AMPK, and PGC-1α in soleus muscle ($n = 4$). Data are expressed as mean ± SD. $^{*}P < 0.05$; $^{**}P < 0.01$.

4. Discussion

Skeletal muscle is a complex structure with multiple functions, a prerequisite for various activities such as maintaining body posture, heat production, and energy metabolism[33-34]. Previous studies have demonstrated that some natural active compounds can act as "exercise mimetics" and benefit the physiological functioning of skeletal muscle. For example, naringin supplementation enhances the expression of slow skeletal muscle fibers, improving exercise endurance and performance[35], whereas geniposide promotes the formation of fast skeletal muscle fibers and improves glucose metabolism[36]. As a representative active ingredient in citrus fruits with high medicinal value, TAN has received much attention in maintaining health due to its high bioavailability and low toxicity.

Our previous study found that TAN regulates skeletal muscle mitochondrial biogenesis and improves endurance performance in mice[15,37]. TAN has also been shown to resist obesity induced by an HFD[13-14]. The expression of irisin as a muscle factor is closely related to skeletal muscle movement[38-39]. The current study has, for the first time, found that TAN has a significant effect on promoting the up-regulation of FNDC5/circulating irisin expression in C2C12 cells and C57BL/6J mice and can counteract the attenuation of FNDC5/circulating irisin expression in obese mice due to an HFD. Additionally, this work explored the potential physiological functions of TAN by activating the SESN2/AMPK/PGC-1α signaling pathway.

PGC-1α is a coactivator that shows significant expression levels in the heart, skeletal muscle, liver, and kidney[40-41]. However, its expression levels fall with an HFD or obesity[42]. PGC1-α is widely acknowledged as a crucial target for addressing type II diabetes mellitus, obesity, and other diseases related to metabolism[43-44]. It is widely accepted that PGC-1α activation is induced by exercise or sustained muscle activity and that PGC-1α upregulates the expression of FNDC5/cyclic irisin[45-46]. In the present study, TAN upregulated PGC-1α protein expression in C2C12 myotubular cells, C57BL/6J mice, and HFD-induced obese mice. This suggests that TAN's increase in FNDC5/circulating irisin expression may be achieved by the process of PGC-1α. AMPK, a receptor for intracellular energy changes, is involved in glucose, fatty acids, and mitochondria-related activities and is one of the main proteins in skeletal muscle[47-48]. The AMPK/PGC-1α signaling pathway is a critical pathway for mitochondrial biosynthesis, and studies have demonstrated that the phosphorylated expression of AMPK upregulates the expression of PGC-1α protein[49]. PGC-1α is a downstream target molecule of AMPK. Furthermore, the AMPK/PGC-1α pathway significantly impacts skeletal muscle, encompassing growth, development, and physiological and pathological functions[15,50]. This study found a significant increase in the expression of p-AMPK and PGC-1α in C2C12 myotubular cells and mice compared to the control group. This suggests that TAN may regulate the expression of FNDC5/cyclic irisin through the AMPK/PGC-1α pathway.

SESN2 is a highly conserved stress-inducible protein that can regulate oxidative stress response and maintain the stability of body functions by activating AMPK[51-52]. Exercise is an effective means to improve skeletal muscle function, and several studies have reported that exercise promotes skeletal muscle SESN2 expression and improves muscle function and exercise capacity[53-54]. Therefore, the SESN2/AMPK/PGC-1α signaling pathway may be an important pathway to increase FNDC5/irisin expression. In this study, we predicted the possibility of the interaction of SESN2 with TAN using molecular modeling found that TAN exhibited a promoting effect on SESN2 expression in both C2C12 myotubular cells and skeletal muscle of mice. These results further validate that TAN could enhance the expression of circulating irisin and skeletal muscle FNDC5 by activating the SESN2/AMPK/PGC-1α signaling axis.

Obesity is often accompanied by skeletal muscle dysfunction and disturbances in muscle factor secretion[55]. Multiple studies have demonstrated that obesity induces a decrease in the expression of FNDC5 in skeletal muscle and a reduction in circulating levels of irisin[31-32], which was also confirmed in our experiments. The dysregulation of irisin can result in metabolic disorders, muscle dysfunction, and insulin resistance[5,8,56], which can exacerbate obesity and thereby enter a vicious cycle. In addition, we found that the administration of TAN substantially improved the conditions of obese mice induced by an HFD despite the fact that FNDC5/irisin expression was significantly down-regulated. Furthermore, we found that TAN could resist the SESN2/AMPK/PGC-1α signaling pathway that appeared to be inhibited in the HFD group of mice. This suggests that the potential of TAN as a natural active ingredient for upregulating FNDC5/irisin expression. TAN has been shown to have significant medicinal potential in the treatment of metabolic diseases and obesity in previous studies. It was able to maintain blood glucose concentration and improve glucose metabolism and insulin resistance in diabetic rats, as well as exhibit excellent fat loss in obese mice induced by an HFD[13-14]. Our results further confirmed that TAN may be a potential ingredient for improving obesity, type II diabetes, and other metabolic diseases. Moreover, our findings further revealed that TAN has the potential to upregulate the expression of FNDC5/irisin through the SESN2/AMPK/PGC-1α signaling pathway and resist the reduction of irisin levels in obese mice induced by an HFD.

To summarize, the supplementation of TAN activated the SESN2/AMPK/PGC-1α signaling pathway and resulted in an increase in FNDC5/irisin expression. Furthermore, TAN successfully counteracted the decrease in irisin secretion caused by an HFD and improved glucose and lipid metabolism in obese mice. Therefore, TAN, being a naturally active compound, presents a novel opportunity to improve the condition of irisin deficiency and other metabolic disorders.

Conflicts of interest

Guangning Kou is a youth editorial board member for *Food Science and Human Wellness* and was not involved in the editorial review or the decision to publish this article. The authors declared that they have no conflicts of interest in this work.

Acknowledgements

This study was funded by the National Natural Science Foundation of China (82103831) and Natural Science Foundation of Henan (242300421265).

References

[1] W.R. Frontera, J. Ochala, Skeletal muscle: a brief review of structure and function, Calcif. Tissue Int. 96 (2015) 183-195. https://doi.org/10.1007/s00223-014-9915-y.

[2] B.K. Pedersen, M.A. Febbraio, Muscle as an endocrine organ: focus on muscle-derived interleukin-6, Physiol. Rev. 88 (2008) 1379-1406. https://doi.org/10.1152/physrev.90100.2007.

[3] P. Boström, J. Wu, M.P. Jedrychowski, et al., A PGC1-α-dependent myokine that drives brown-fat-like development of white fat and thermogenesis, Nature 481 (2012) 463-468. https://doi.org/10.1038/nature10777.

[4] T. Zou, S. Li, B. Wang, et al., Curcumin improves insulin sensitivity and increases energy expenditure in high-fat-diet-induced obese mice associated with activation of FNDC5/irisin, Nutrition 90 (2021) 111263. https://doi.org/10.1016/j.nut.2021.111263.

[5] C. Rodriguez Lanzi, D.J. Perdicaro, J. Gambarte Tudela, et al., Grape pomace extract supplementation activates FNDC5/irisin in muscle and promotes white adipose browning in rats fed a high-fat diet, Food Funct. 11 (2020) 1537-1546. https://doi.org/10.1039/c9fo02463h.

[6] L. Lenhare, B.M. Crisol, V.R.R. Silva, et al., Physical exercise increases Sestrin 2 protein levels and induces autophagy in the skeletal muscle of old mice, Exp Gerontol. 97 (2017) 17-21. https://doi.org/10.1016/j.exger.2017.07.009.

[7] S.D. Anton, A. Hida, R. Mankowski, et al., Nutrition and exercise in sarcopenia, Curr. Protein Pept. Sci. 19 (2018) 649-667. https://doi.org/10.2174/1389203717666161227144349.

[8] P.A. Boström, J.M. Fernández-Real, Metabolism: irisin, the metabolic syndrome and follistatin in humans, Nat. Rev. Endocrinol. 10 (2014) 11-12. https://doi.org/10.1038/nrendo.2013.230.

[9] Q. Zhou, K. Chen, P. Liu, et al., Dihydromyricetin stimulates irisin secretion partially *via* the PGC-1α pathway, Mol. Cell. Endocrinol. 412 (2015) 349-357. https://doi.org/10.1016/j.mce.2015.05.036.

[10] E.S.A. Arafa, Q. Zhu, B.M. Barakat, et al., Tangeretin sensitizes cisplatin-resistant human ovarian cancer cells through downregulation of phosphoinositide 3-kinase/Akt signaling pathway, Cancer Res. 69 (2009) 8910-8917. https://doi.org/10.1158/0008-5472.CAN-09-1543.

[11] C.C. Li, H.J. Hsu, Y.S. Wang, et al., Effects of heat treatment on the antioxidative and anti-inflammatory properties of orange by-products, Food Funct. 8 (2017) 2548-2557. https://doi.org/10.1039/c7fo00188f.

[12] K.P. Datla, M. Christidou, W.W. Widmer, et al., Tissue distribution and neuroprotective effects of citrus flavonoid tangeretin in a rat model of Parkinson's disease, Neuroreport 12 (2001) 3871-3875. https://doi.org/10.1097/00001756-200112040-00053.

[13] Q. Chen, D. Wang, Y. Gu, et al., Tangeretin prevents obesity by modulating systemic inflammation, fat browning, and gut microbiota in high-fat diet-induced obese C57BL/6 mice, J. Nutr. Biochem. 101 (2022) 108943. https://doi.org/10.1016/j.jnutbio.2022.108943.

[14] R. Sundaram, P. Shanthi, P. Sachdanandam, Effect of tangeretin, a polymethoxylated flavone on glucose metabolism in streptozotocin-induced diabetic rats, Phytomedicine 21 (2014) 793-799. https://doi.org/10.1016/j.phymed.2014.01.007.

[15] G. Kou, Z. Li, C. Wu, et al., Citrus tangeretin improves skeletal muscle mitochondrial biogenesis *via* activating the AMPK-PGC1-α pathway *in vitro* and *in vivo*: a possible mechanism for its beneficial effect on physical performance, J. Agric. Food Chem. 66 (2018) 11917-11925. https://doi.org/10.1021/acs.jafc.8b04124.

[16] J. Matsuda, A. Takahashi, Y. Takabatake, et al., Metabolic effects of RUBCN/Rubicon deficiency in kidney proximal tubular epithelial cells, Autophagy 16 (2020) 1889-1904. https://doi.org/10.1080/15548627.2020.1712107.

[17] L. Ding, Q. Yang, E. Zhang, et al., Notoginsenoside Ft1 acts as a TGR5 agonist but FXR antagonist to alleviate high fat diet-induced obesity and insulin resistance in mice, Acta Pharm. Sin B. 11 (2021) 1541-1554. https://doi.org/10.1016/j.apsb.2021.03.038.

[18] R. Salomon-Ferrer, D.A. Case, R.C. Walker, An overview of the Amber biomolecular simulation package, WIREs Comput. Mol. Sci. 3 (2013) 198-210. https://doi.org/10.1002/wcms.1121.

[19] C. Sagui, T.A. Darden, Molecular dynamics simulations of biomolecules: long-range electrostatic effects, Annu. Rev. Biophys. Biomol. Struct. 28 (1999) 155-179. https://doi.org/10.1146/annurev.biophys.28.1.155.

[20] V. Kräutler, W.F. van Gunsteren, P.H. Hünenberger, A fast SHAKE algorithm to solve distance constraint equations for small molecules in molecular dynamics simulations, J. Comput. Chem. 22 (2001) 501-508. https://doi.org/10.1002/1096-987X(20010415)22:5<501::AID-JCC1021>3.0.CO;2-V.

[21] L. Larini, R. Mannella, D. Leporini, Langevin stabilization of molecular-dynamics simulations of polymers by means of quasisymplectic algorithms, J. Chem. Phys. 126 (2007) 104101. https://doi.org/10.1063/1.2464095.

[22] Y. Chen, Y. Zheng, P. Fong, et al., The application of the MM/GBSA method in the binding pose prediction of FGFR inhibitors, Phys. Chem. Chem. Phys. 22 (2020) 9656-9663. https://doi.org/10.1039/d0cp00831a.

[23] T. Hou, J. Wang, Y. Li, et al., Assessing the performance of the MM/PBSA and MM/GBSA methods. 1. The accuracy of binding free energy calculations based on molecular dynamics simulations, J. Chem. Inf. Model. 51 (2011) 69-82. https://doi.org/10.1021/ci100275a.

[24] S. Genheden, U. Ryde, The MM/PBSA and MM/GBSA methods to estimate ligand-binding affinities, Expert. Opin. Drug. Discov. 10 (2015) 449-461. https://doi.org/10.1517/17460441.2015.1032936.

[25] L. Feng, B. Li, M. Cai, et al., Resistance exercise alleviates the prefrontal lobe injury and dysfunction by activating SESN2/AMPK/PGC-1α signaling pathway and inhibiting oxidative stress and inflammation in mice with myocardial infarction, Exp. Neurol. 370 (2023) 114559. https://doi.org/10.1016/j.expneurol.2023.114559.

[26] J. Sun, F.H. Song, J.Y. Wu, et al., Sestrin2 overexpression attenuates osteoarthritis pain *via* induction of AMPK/PGC-1α-mediated mitochondrial biogenesis and suppression of neuroinflammation, Brain Behav. Immun. 102 (2022) 53-70. https://doi.org/10.1016/j.bbi.2022.02.015.

[27] X. Hu, Z. Zeng, J. Zhang, et al., Molecular dynamics simulation of the interaction of food proteins with small molecules, Food Chem. 405 (2023) 134824. https://doi.org/10.1016/j.foodchem.2022.134824.

[28] S. Decherchi, A. Cavalli, Thermodynamics and kinetics of drug-target binding by molecular simulation, Chem. Rev. 120 (2020) 12788-12833. https://doi.org/10.1021/acs.chemrev.0c00534.

[29] C. Cen, J. Chen, W. Wang, et al., Exploring the interaction mechanism of dietary protein ovalbumin and folic acid: a combination research of molecular simulation technology and multispectroscopy, Food Chem. 385 (2022) 132536. https://doi.org/10.1016/j.foodchem.2022.132536.

[30] E. Wang, H. Sun, J. Wang, et al., End-point binding free energy calculation with MM/PBSA and MM/GBSA: strategies and applications in drug design, Chem. Rev. 119 (2019) 9478-9508. https://doi.org/10.1021/acs.chemrev.9b00055.

[31] A. Guo, K. Li, H.C. Tian, et al., FGF19 protects skeletal muscle against obesity-induced muscle atrophy, metabolic derangement and abnormal irisin levels *via* the AMPK/SIRT-1/PGC-α pathway, J. Cell. Mol. Med. 25 (2021) 3585-3600. https://doi.org/10.1111/jcmm.16448.

[32] S. Shen, Q. Liao, T. Zhang, et al., Myricanol modulates skeletal muscle-adipose tissue crosstalk to alleviate high-fat diet-induced obesity and insulin resistance, Br. J. Pharmacol. 176 (2019) 3983-4001. https://doi.org/10.1111/bph.14802.

[33] J.M. Argilés, N. Campos, J.M. Lopez-Pedrosa, et al., Skeletal muscle regulates metabolism *via* interorgan crosstalk: roles in health and disease, J. Am. Med. Dir. Assoc. 17 (2016) 789-796. https://doi.org/10.1016/j.jamda.2016.04.019.

[34] J.R. Zierath, J.A. Hawley, Skeletal muscle fiber type: influence on contractile and metabolic properties, PLoS Biol. 2 (2004) e348. https://doi.org/10.1371/journal.pbio.0020348.

[35] P. Li, S. Zhang, H. Song, et al., Naringin promotes skeletal muscle fiber remodeling by the AdipoR1-APPL1-AMPK signaling pathway, J. Agric. Food. Chem. 69 (2021) 11890-11899. https://doi.org/10.1021/acs.jafc.1c04481.

[36] Y. Li, H. Pan, X. Zhang, et al., Geniposide improves glucose homeostasis *via* regulating FoxO1/PDK4 in skeletal muscle, J. Agric. Food Chem. 67 (2019) 4483-4492. https://doi.org/10.1021/acs.jafc.9b00402.

[37] J. Li, J. Li, A. Ullah, et al., Tangeretin enhances muscle endurance and aerobic metabolism in mice *via* targeting AdipoR1 to increase oxidative myofibers, J. Agric. Food Chem. 72 (2024) 16687-16699. https://doi.org/10.1021/acs.jafc.3c09386.

[38] S. Qiu, E. Bosnyák, G. Treff, et al., Acute exercise-induced irisin release in healthy adults: associations with training status and exercise mode, Eur. J. Sport Sci. 18 (2018) 1226-1233. https://doi.org/10.1080/17461391.2018.1478452.

[39] N. Uysal, O. Yuksel, S. Kizildag, et al., Regular aerobic exercise correlates with reduced anxiety and incresed levels of irisin in brain and white adipose tissue, Neurosci. Lett. 676 (2018) 92-97. https://doi.org/10.1016/j.neulet.2018.04.023.

[40] P. Puigserver, Z. Wu, C.W. Park, et al., A cold-inducible coactivator of nuclear receptors linked to adaptive thermogenesis, Cell 92 (1998) 829-839. https://doi.org/10.1016/s0092-8674(00)81410-5.

[41] R.B. Vega, J.L. Horton, D.P. Kelly, Maintaining ancient organelles: mitochondrial biogenesis and maturation, Circ. Res. 116 (2015) 1820-1834. https://doi.org/10.1161/CIRCRESAHA.116.305420.

[42] C. Handschin, B.M. Spiegelman, The role of exercise and PGC1α in inflammation and chronic disease, Nature 454 (2008) 463-469. https://doi.org/10.1038/nature07206.

[43] Y. Cho, B.C. Hazen, A.P. Russell, et al., Peroxisome proliferator-activated receptor γ coactivator 1 (PGC-1)- and estrogen-related receptor (ERR)-induced regulator in muscle 1 (Perm1) is a tissue-specific regulator of oxidative capacity in skeletal muscle cells, J. Biol. Chem. 288 (2013) 25207-25218. https://doi.org/10.1074/jbc.M113.489674.

[44] M.E. Patti, A.J. Butte, S. Crunkhorn, et al., Coordinated reduction of genes of oxidative metabolism in humans with insulin resistance and diabetes: potential role of PGC1 and NRF1, PNAS 100 (2003) 8466-8471. https://doi.org/10.1073/pnas.1032913100.

[45] N. Perakakis, G.A. Triantafyllou, J.M. Fernández-Real, et al., Physiology and role of irisin in glucose homeostasis, Nat. Rev. Endocrinol. 13 (2017) 324-337. https://doi.org/10.1038/nrendo.2016.221.

[46] L.I. Arhire, L. Mihalache, M. Covasa, Irisin: a hope in understanding and managing obesity and metabolic syndrome, Front. Endocrinol. 10 (2019) 524. https://doi.org/10.3389/fendo.2019.00524.

[47] D.G. Hardie, K. Sakamoto, AMPK: a key sensor of fuel and energy status in skeletal muscle, Physiology 21 (2006) 48-60. https://doi.org/10.1152/physiol.00044.2005.

[48] H.M. O'Neill, G.P. Holloway, G.R. Steinberg, AMPK regulation of fatty acid metabolism and mitochondrial biogenesis: implications for obesity, Mol. Cell. Endocrinol. 366 (2013) 135-151. https://doi.org/10.1016/j.mce.2012.06.019.

[49] H.M. O'Neill, S.J. Maarbjerg, J.D. Crane, et al., AMP-activated protein kinase (AMPK) β1β2 muscle null mice reveal an essential role for AMPK in maintaining mitochondrial content and glucose uptake during exercise, PNAS 108 (2011) 16092-16097. https://doi.org/10.1073/pnas.1105062108.

[50] L.L. Ji, D. Yeo, C. Kang, Muscle disuse atrophy caused by discord of intracellular signaling, Antioxid. Redox. Signal 33(11) (2020) 727-744. https://doi.org/10.1089/ars.2020.8072.

[51] Q. Lin, Y. Ma, Z. Chen, et al., Sestrin-2 regulates podocyte mitochondrial dysfunction and apoptosis under high-glucose conditions *via* AMPK, Int. J. Mol. Med. 45 (2020) 1361-1372. https://doi.org/10.3892/ijmm.2020.4508.

[52] X. Han, C. Ding, G. Zhang, et al., Liraglutide ameliorates obesity-related nonalcoholic fatty liver disease by regulating Sestrin2-mediated Nrf2/HO-1 pathway, Biochem. Biophys. Res. Commun. 525 (2020) 895-901. https://doi.org/10.1016/j.bbrc.2020.03.032.

[53] Y. Huang, C. Jiang, X. Li, et al., Resistance exercise preconditioning prevents disuse muscle atrophy by inhibiting apoptosis and protein degradation *via* SESN2 in C57BL/6J mice, Biochim. Biophys. Acta. Mol. Basis. Dis. 1870 (2024) 167111. https://doi.org/10.1016/j.bbadis.2024.167111.

[54] Y. Yang, X. Yang, Y. Huang, et al., Resistance exercise alleviates dexamethasone-induced muscle atrophy *via* Sestrin2/MSTN pathway in C57BL/6J mice, Exp. Cell Res. 432 (2023) 113779. https://doi.org/10.1016/j.yexcr.2023.113779.

[55] H. Wu, C.M. Ballantyne, Skeletal muscle inflammation and insulin resistance in obesity, J. Clin. Invest. 127 (2017) 43-54. https://doi.org/10.1172/JCI88880.

[56] M. Guo, J. Yao, J. Li, et al., Irisin ameliorates age-associated sarcopenia and metabolic dysfunction, J. Cachexia. Sarcopeni. 14 (2022) 391-405. https://doi.org/10.1002/jcsm.13141.